Journal Name

ARTICLE TYPE

Cite this: DOI: 10.1039/xxxxxxxxxx

Supporting Information for *Fabrication of micro-scaled materials with programmable composition gradients*

Cédric Laval,[a] Anne Bouchaudy,[a] and Jean-Baptiste Salmon*[a]

Received Date
Accepted Date

DOI: 10.1039/xxxxxxxxxx

www.rsc.org/journalname

Pervaporation-induced growth of materials

The pervaporation-induced flow convects the solutes or the particles contained in the reservoirs up to the formation and growth of a dense material, see Fig. 1c (left) in the main text. Two limiting cases may arise depending on the chemical nature of the solutes.

For a dilute colloidal dispersion, the growing material is a porous packed bed of colloids through which water flows and can thus pervaporate, see Fig. S1. The pervaporation-induced flow thus still obeys eqn (1), and the incoming flux of colloids remains constant: $\phi_0 v_0 = -\phi_0 L_0/\tau_e$, ϕ_0 being the volume fraction of colloids in the reservoir. Solute conservation then implies that the growth of the material follows:

$$\phi_d \dot{x}_d \approx -\phi_0 v_0 \,, \tag{S1}$$

i.e. a constant growth rate owing to the constant incoming flux of colloids (ϕ_d is the volume fraction of the packed bed). Actually, the above conservation equation is only an approximation of a non-linear relation which takes into account the shape of the concentration profile upstream of the material[1]. Deviations are however only significant at early time scales and/or for large ϕ_0, see Fig. S1a.

For an aqueous molecular solution (surfactants, polymers, etc.), the increase of the solute concentration at the tip of the channel decreases the chemical activity of water, and thus slows down the driving force for pervaporation across the membrane[2]. In this case, concentration increases up to the formation of a dry material ($\phi \to 1$) which does not contribute anymore to the pervaporation process, see Fig. S1b. The dry material therefore shifts the pervaporation-induced flow which now follows:

$$v(x) = -q_e(x - x_d)/(hw) = -(x - x_d)/\tau_e \,. \tag{S2}$$

The incoming flux of solutes decreases as the material invades the channel, see Fig. S1b. Solute conservation in this case is $\dot{x}_d \approx -\phi_0 v_0 (1 - x_d/L_0)$, leading to a growth which slows down exponentially:

$$x_d/L_0 \approx 1 - \exp(-\phi_0 (t - \tau_n)/\tau_e) \,. \tag{S3}$$

τ_n corresponds to the *induction* time of the dry material and is given by the complete resolution of the concentration dynamics[3].

The above two regimes were reported experimentally for various systems even with quantitative agreements with eqns (S1) and (S3)[1,4]. The agreement is only semi-quantitative for dispersions of small nanoparticles (radii < 50 nm) and polymer inks, because the solidification of the solution/dispersion within the channels deforms significantly the PDMS matrix[5,6]. In this case, the growth dynamics follow nevertheless either a linear growth eqn (S1) or an exponential slowdown eqn (S3), but with empirical parameters to account for the deformations[3].

Microfabrication

Master templates– To combine both push-down valves and a static herringbone mixer, we use standard protocols[7] to fabricate master templates with rounded channels at the level of the inlets and rectangular channels everywhere else, see the SEM image shown in Fig. 1c in the main text. Two-level rectangular channels are obtained using standard aligment processes and the successive photopatterning of negative photoresists (SU-8 3025 and SU-8 3005, MicroChem). Rounded channels are obtained using a positive photoresist (AZ 40 XT, AZ Electronic Materials) which is melted

---

[a] *CNRS, Solvay, LOF, UMR 5258, Univ. Bordeaux, F-33600 Pessac, France. E-mail: jean-baptiste.salmon-exterieur@solvay.com*

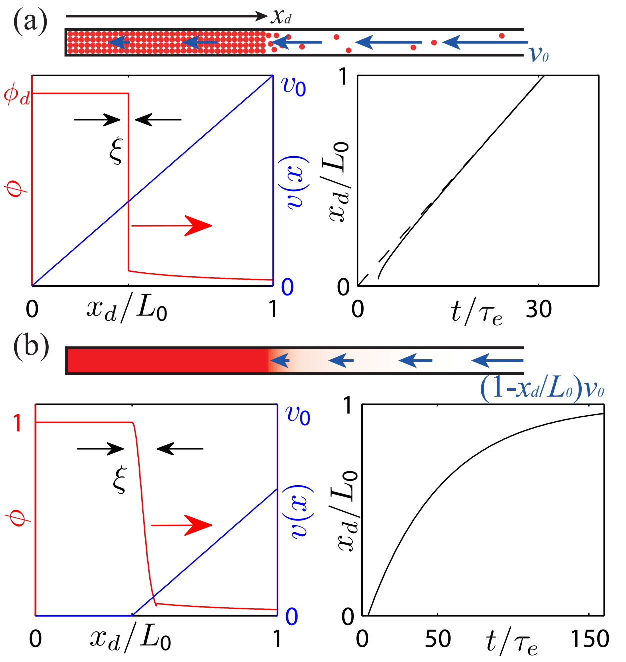

Fig. S1 (a) Growth of a packed bed of colloids. Left: concentration profile (red, front width ξ) and pervaporation-induced flow (blue). Right: growth dynamics x_d vs. t given by eqn (S1) (dotted line). The continuous line is the full theoretical prediction of ref.[1] for $\phi_0 = 0.02$ and $\phi_d = 0.64$. (b) Growth of a dry material. Pervaporation ceases within the material and the incoming flux decreases. Left: concentration profile (red) and pervaporation-induced flow *shifted* by the growing material, see eqn (S2) (blue). Right: growth dynamics x_d vs. t given by eqn (S3) for $\phi_0 = 0.02$.

and reflowed by heating after photopatterning. The heights of the channels were measured using a surface profiler (Dektak, Veeco): $H = 25$ μm, $h = 35$ μm, and $h_0 = 10$ μm see Fig. 1c in the main text, and the widths of the channels are $w = 100$ μm and $W = 300$ μm (after reflow).

The control channels and the channels for the flow of dry air were fabricated using a SU-8 master template of height 60 μm (see the real design displayed in Fig. S2). The width of the control channels is 300 μm and 600 μm for the channels overlapping the pervaporation channels.

Multilayer soft lithography– A thin PDMS layer (Sylgard 184, Dow Corning, thickness 50 μm) is spin-coated on the first mold containing the fluidic channels and left to reticulate at high temperature (65°C, 45 min). A thick PDMS layer is poured onto the second master (control channels) and after complete reticulation, this elastomeric stamp is aligned and bounded on the PDMS membrane deposited on the first mold (plasma cleaning, Diener Electronic). The whole PDMS device is then carefully peeled off the template, punched to create access holes, and bounded on a glass slide previously spin-coated by a thin PDMS layer (≈ 50 μm).

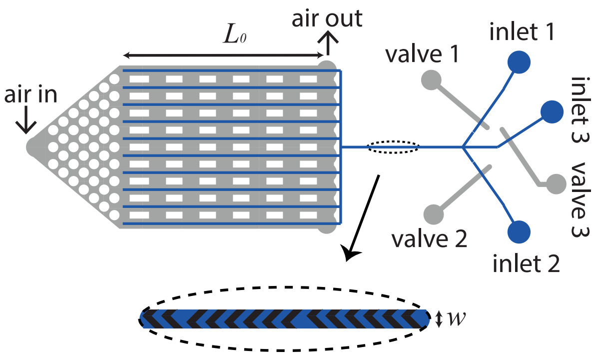

Fig. S2 Real microfluidic design of the chip shown schematically in Fig. 1 in the main text. The reservoirs (3 in the present case) are connected to 10 parallel pervaporation channels and are controlled by three independent valves. The zoom evidences the staggered herringbone mixer upstream of the pervaporation area. The approximate dimensions of the chip are 3.5×1.5 cm^2 and 6 identical units were made on a single 4" wafer using lithography.

Movies

Movie *BarCode.avi* **–** Movie corresponding to the experiment reported in fig. 4a in the main text. Channel width $w = 100$ μm. Time interval between two successive frames $\Delta t = 125$ s. The blinking at low frequency is due to slow temporal modulations of the mercury lamp.

Movie *ContinuousGradient.avi* **–** Movie corresponding to the experiment reported in fig. 4b in the main text. Channel width $w = 100$ μm. Time interval between two successive frames $\Delta t = 250$ s. The blinking at low frequency is due to slow temporal modulations of the mercury lamp.

Calculation of $r(t)$ for polymeric materials

For polymer solutions, the pervaporation-induced flow leads to the growth of a dry material which does not contribute anymore to pervaporation (see Fig. S1). The pervaporation-induced flow is thus shifted upstream of the material, and the growth dynamics follows an exponential slowing down, see eqns. (S2) and (S3). Despite this slowing down, it is always possible to calculate the trajectory $x_t(t,t_0)$ of a thin stripe of liquid emerging from the valves at $t = t_0$, knowing both $v(x,t)$ and the growth dynamics $x_d(t)$. More precisely, we solved the following ordinary differential equation (Matlab):

$$\frac{\mathrm{d}x_t}{\mathrm{d}t} = v(x_t,t), \tag{S4}$$

with

$$v(x_t) = -(x_t - x_d)/\tau_e \quad \text{for} \quad x_t < L_0 \tag{S5}$$

$$x_d(t)/L_0 = 1 - \exp(-(t-\tau_n)/\tau_g)\,. \tag{S6}$$

τ_n and τ_g are both parameters estimated by fitting the experimental growth dynamics, see Fig. 5b in the main text. In the case of the exact geometry of the chip depicted Fig. 1 above, trajectories $x_t(t,t_0)$ were calculated for the central pervaporation channel only, and we took into account the transit from the valves up to the pervaporation area using a constant velocity $v(x) = (L_0 - x_d)/\tau_e$ for $x_t > L_0$ over a length $l/10$, with l the geometrical distance between the valves and the entrance of the channel (the factor 10 comes from the 10 times increase of the pervaporation-induced flow rate in the upstream fluidic channel connected to the 10 parallel pervaporation channels). The initial condition of this ordinary differential equation is thus $x_t(t_0,t_0) = L_0 + l/10$.

Knowledge of the trajectories $x_t(t,t_0)$ enables us to relate the positions $x_t(t \to \infty, t_0)$ within the dry material to the times t_0 at which the corresponding liquid stripes emerge from the valves. Finally, the same relation is used to relate the expected continuous gradient $r(x)$ along the dry material to the temporal evolution $r(t_0)$ of the ratio of opening of valves A and B, with $x = x_t(t \to \infty, t_0)$ calculated as above, see Fig. 5 in the main text.

References

1 A. Merlin, J.-B. Salmon and J. Leng, *Soft Matter*, 2012, **8**, 3526–3537.

2 M. Schindler and A. Ajdari, *Eur. Phys. J E*, 2009, **28**, 27–45.

3 C. Laval, P. Poulin and J.-B. Salmon, *Soft Matter*, 2016, **12**, 1810.

4 J. Angly, A. Iazzolino, J.-B. Salmon, J. Leng, S. Chandran, V. Ponsinet, A. Desert, A. L. Beulze, S. Mornet, M. Treguer-Delapierre and M. Correa-Duarte, *ACS Nano*, 2013, **7**, 6465–6477.

5 N. Ziane and J.-B. Salmon, *Langmuir*, 2015, **31**, 7943–7952.

6 M. T. Demko, T. P. Brackbill and A. P. Pisano, *Langmuir*, 2012, **28**, 9857–9863.

7 P. M. Fordyce, C. A. Diaz-Botia, J. L. DeRisi and R. Gomez-Sjoberg, *Lab Chip*, 2012, **12**, 4287–4295.